ORIGINAL ARTICLE

Development and preclinical assessment of nanoemulgel loaded with phytoconstituents for the management of rheumatoid arthritis

Anita Chando[1] · Vivek Basudkar[1] · Sankalp Gharat[1] · Munira Momin[1,2] · Tabassum Khan[3]

Abstract

In recent years, natural ingredients have gained importance for therapeutic treatment due to their minimal toxicity. However, the delivery of these phytoconstituents poses a challenge to provide better efficacy. Current research reports the development of nanoemulgel (NEG) loaded with ginger oleoresin (GOR) and lipid guggul extract (LGE) for the management of rheumatoid arthritis (RA). The nanoemulsion (NE) was developed using the spontaneous emulsification technique by the pseudo-ternary method. The optimized nanoemulsion exhibited globule size of 16.08 ± 2.55 nm, PDI of 0.187 ± 0.06, and zeta potential of -22.4 ± 0.31 mV. The cumulative release from in vitro diffusion studies at pH 7.4 was about $99.72 \pm 3.47\%$, $57.98 \pm 2.11\%$, and $86.42 \pm 5.13\%$ of 6-gingerol, E-guggulsterone, and Z-guggulsterone respectively at the end of 24 h. The ex vivo studies on porcine ear skin showed sustained release with $92.8 \pm 3.21\%$ for 6-gingerol, $55.61 \pm 0.91\%$ for E-guggulsterone, and $84.2 \pm 4.22\%$ for Z-guggulsterone released at the end of 24 h. The cell culture studies on RAW 264.7 cells indicated a robust inhibition of LPS-induced IL-6 and TNF-α production indicating its efficacy in the management of RA. The preclinical studies on male Wistar rats suggest that the developed NEG exhibited a comparable decrease in paw edema inflammation as compared to the marketed diclofenac sodium gel. These encouraging results demonstrate the potential of the developed nanoemulgel containing combination of GOR and LGE for the management of RA.

Keywords Nanoemulgel · Rheumatoid arthritis · Ginger oleoresin · Lipid guggul extract

Introduction

Rheumatoid arthritis (RA) is a chronic immune-mediated disorder characterized by persistent inflammation, swelling, and stiffness of joints due to synovial hyperplasia and pannus formation [1, 2]. According to WHO reports, generally, RA develops between age of 20 and 40 being the most productive age of humans that often leads to pain, deformity and chronic disabling conditions and loss of quality life [3]. Young children below the age of 16 years having RA are referred to as juvenile rheumatoid arthritis (JRA) [4, 5]. Recent epidemiological study shows that the prevalence of RA is about 0.24–1% in developed countries and affects a greater number of women (2–3 times) than men. The RA may be diagnosed as early as 3 months from onset to 2 years when the disease is established [6]. Progression of RA is associated with difficulties in the day-to-day activities, leading to physical disability. A recent survey demonstrated that within 10 years of onset of RA, more than 50% patients in developed countries discontinued from a full time job [3].

Rheumatoid arthritis develops in patients due to various factors comprising of genetic and/or environment. Cytokine and T cell signaling plays a critical role in the progression of RA [7]. The synovial inflammation and articular destruction associated with RA are characterized by elevated levels of pro-inflammatory cytokines such as IL-6, IL-1β, and tumor necrosis factor (TNF-α) along with prostaglandin E2 (PGE2) and nitric oxide (NO). It has been observed that the level of pro-inflammatory cytokines is more than compared to

Anita Chando and Vivek Basudkar contributed equally to this work.

✉ Munira Momin
munira_momin@yahoo.com

1 Department of Pharmaceutics, SVKM's Dr. Bhanuben Nanavati College of Pharmacy, Mumbai, Maharashtra, India

2 SVKM's Shri C. B. Patel Research Centre for Chemistry and Biological Sciences, Vile Parle (West), Mumbai, Maharashtra, India

3 Department of Pharmaceutical Chemistry, SVKM's Dr. Bhanuben Nanavati College of Pharmacy, Mumbai, Maharashtra, India

anti-inflammatory cytokines in patients with RA; this further accelerates the activity of other cytokines leading to destruction of bone and cartilage. IL-1 is one of the primary pro-inflammatory cytokines secreted by synovial macrophages, which plays significant role in progression of RA by exerting multiple biological effects such as synthesis of collagenase, prostaglandin (PG), stimulation of fibroblasts, and chemotaxis for B and T cells. TNF-α is another important cytokine, which is abundantly found in the rheumatoid joints as well as circulation and stimulates PGE2 and collagenase, induces bone resorption, and inhibits bone formation and production of matrix metalloproteinases (MMPs) [3, 8]. Recent developments in the technology of diagnostic have helped to detect and understand the underlying mechanism of RA; however, the exact pathology is still unknown [9].

Currently, RA treatment modalities provide symptomatic relief that includes anti-inflammation medicines, steroids, analgesics, disease-modifying anti-rheumatic drugs, (DMARDs) and monoclonal antibodies (MAbs). Nonetheless, these drugs also have plenty of adverse effects, including digestive problems, renal toxicity, loss of protein, toxicity, and immunosuppressive effects, all of which contribute to poor patient compliance [10, 11]. As a result, plant-based treatments are now being explored for the management of rheumatoid arthritis. Ginger oleoresin (GOR) contains shagoals and gingerols, which are found to inhibit cyclooxygenase 2 (COX-2), because of which it possesses anti-inflammatory property. 6-Gingerol is also known to inhibit prostaglandin (PG) and leukotriene biosynthesis through suppression of 5-lipoxygenase (5-LOX) and PG synthetase. Further inhibition of synthesis of the pro-inflammatory cytokines such as IL-1β, IL-6, and TNF-α leads to the anti-inflammatory activity [12, 13]. Lipid guggul extract (LGE) is reported for anti-inflammatory activity by ameliorating the levels of pro-inflammatory mediators such as IL-6, TNF-α, IL-1β, NO, IL-12, and IFN-γ. E- and Z-guggulsterones decrease the levels of pro-inflammatory cytokines like IL-1β, IL-2, and TNF-α and suppress cyclooxygenase-2 (COX-2) mRNA levels, which thereby demonstrates anti-inflammation and anti-arthritic activity [14, 15]. Both the active phytoconstituents are lipophilic in nature; hence, delivering in the form of nanoemulsion can increase their efficacy and suppress side effects in the management of RA.

Nanoemulsion (NE) is a biphasic colloidal dispersion of two immiscible liquids that are thermokinetically stable and thermodynamically unstable. NE has a lipidic interior and is a good choice for delivering and improving the bioavailability of lipophilic or hydrophobic drugs/extracts. In NE, Brownian motion dominates gravitational forces due to their smaller droplet size, thereby favoring a high kinetic stability towards flocculation, interface deformation, coalescence, etc. NE are preferred choice for drug delivery due to smaller-sized droplets, which therefore provides greater surface area and greater absorption. In addition, they have high drug loading capacity, provide sustained or controlled release, and have higher drug penetration properties [16–19]. However, low viscosity of nanoemulsion leads to low retention rate at the site of application [20]. Hence, NE is incorporated into gel to overcome the drawbacks. In the present study, nanoemulsion was formulated using emulsification technique by the pseudo-ternary method containing GOR and LGE for the therapeutic treatment of RA. Furthermore, nanoemulsion was incorporated into carbopol gel to form nanoemulgel. The developed formulation was evaluated on various parameters including in vitro diffusion studies, ex vivo permeation studies, HET CAM's studies, and preclinical studies on CFA-induced Wistar rats RA model.

Materials and methods

Ginger oleoresin (GOR) and fenugreek oil were kindly gifted from Sunpure Extracts Pvt Ltd, Delhi, India. Lipid guggul extract (LGE) was received as a gift sample from Arjuna Naturals Pvt Ltd, Kerala, India. Castor oil and Capmul MCM were gifted from Jayant Agro-Organic Ltd, Mumbai, India, and Abitec Corporation, USA, respectively. Tween 80 and Kolliphor EL were given as a gift sample from Mohini Organics, Ltd, India, and BASF, Mumbai, India, respectively. Carbopol Ultrez 10 NF was provided as a gift sample from Lubrizol Advanced Materials India Pvt Ltd. Oleic acid, Transcutol P, and Propylene glycol were purchased from Otto Chemie Pvt Ltd, Mumbai. India.

Formulation development

Screening of oils, surfactants, and co-surfactants

As GOR and LGE are liquids, selection of oil phase and surfactant phase was determined on the miscibility of these active phytoconstituents in numerous oils, surfactants, and co-surfactants. Castor oil and fenugreek oil were selected as functional excipients as they are known for anti-inflammatory activity [21, 22]. However, these oils were not sufficient to form a clear and stable nanoemulsion. Therefore, various oils such as isopropyl myristate (IPM), oleic acid (OA), ethyl oleate (EO), Captex 200P (C-200P), and Capmul MCM (C-MCM) were screened to find the optimum ratio of oil mixture. Apart from this, other surfactants and co-surfactants such as Transcutol P (TP), PEG-400, Tween 20 (T20), Tween 80 (T80), Span 80 (S80), Propylene glycol (PG), and Kolliphor ELP (K-ELP) were examined for selection of an appropriate S-mix ratio.

Selection of oil mixture

Miscibility studies were performed using the procedure mentioned in [23] with few modifications. Mixture of 2% wt GOR and 2% wt LGE (1:1) was added to individual oil and various oil mixture (1:1) ratio, vortexed, and allowed to stand for 48 h. After 48 h, it was examined for color change, turbidity, and phase separation. Clear and uniphasic oil mixture was selected and further studied with different surfactant mixtures. Castor oil and fenugreek oil were kept constant throughout the selection procedure as they are the functional excipients.

Selection of surfactant mixture

Mixture of 2% wt GOR and 2% wt LGE (1:1) was added to individual surfactant and surfactant mixture in 1:1 ratio and allowed to stand for 48 h. After 48 h, it was examined for color change, turbidity, and phase separation. Clear and uniphasic surfactant mixes were taken further for constructing pseudo-ternary phase diagrams.

Construction of pseudo-ternary phase diagram

The nanoemulsion area was identified by the construction of pseudo-ternary phase diagrams by water titration method [24]. Based on miscibility studies, different Oil-mix and S-mix were selected while purified water was used as an aqueous phase. The selected surfactants and co-surfactant were mixed (S-mix) in three ratios such as 1:1 and 1:2 to identify the optimal ratio that can result in forming maximum nanoemulsion area. Briefly, the Oil-mix and S-mix were vortexed in various ratios 9:1, 8:2, 7:3, 6:4, 5:5, 4:6, 3:7, 2:8, and 1:9 followed by drop-wise water titration until phase separation or turbidity was observed. Furthermore, the pseudo-ternary phase diagrams were constructed using Chemix school-Portable Chemistry software 7.0 by calculating the percent of Oil-mix, S-mix, and water. Likewise, other ratios of S-mix and the zones for clear and stable nanoemulsion were identified.

Formulation of oil-in-water nanoemulsion

Mixture of 1% wt GOR and 1% wt LGE was added to the selected Oil-mix and S-mix ratios selected from the pseudo-ternary phase diagram of highest nanoemulsion region. The required amount of purified water was added dropwise with continuous stirring at ambient temperature. All the batches were stored at ambient temperature for further evaluation [25].

Characterization and evaluation of nanoemulsion

Physical appearance, surface morphology, droplet size, zeta potential, and polydispersity index

The nanoemulsion formulation was inspected visually for their color, homogeneity, and clarity. Surface morphology of nanoemulsion was studied by using a transmission electron microscope. The mean droplet size (MDS) is based on photon correlation spectroscopy principle that determines the fluctuation in light scattering from Brownian movement of the particles. The MDS was determined using Zetasizer (Nano-ZS, Malvern) Instrument. The PDI ranges from 0 to 1, where 0 to 1 represents a monodisperse to polydisperse particle system. The test samples were diluted in the ratio of 1:100 using purified water. The measurements were made in 90 °C angle at 25 °C in triplicate; mean value and standard deviation were reported [26, 27].

Zeta potential

Zeta potential was determined based on the electrophoretic mobility using Zetasizer (Nano-ZS, Malvern) Instrument. It helps in predicting dispersion stability which is dependent on properties of drug, excipients concentration and presence of electrolytes. The test samples were diluted in the ratio of 1:100 using purified water [28].

Thermodynamic stability and stress testing (centrifugation, heat-cool cycle, and freeze-thaw cycle)

The optimized batches based on pseudo-ternary plots were further subjected to thermodynamic stability. The interfacial film strength was determined by testing the stability of emulsion under centrifugation. Phase separation was observed after centrifugation of the optimized formulation at 4500 rpm for 20 min. Formulations that were stable in centrifugation test were subjected to heat-cool cycle. In heat-cool cycle, the formulations were kept between 4 and 45 °C for six cycles for not less than 48 h and observed visually for any physical changes. The stable formulations were further evaluated in freeze-thaw cycles. Three freeze-thaw cycles between − 21 and 25 °C were performed at each temperature for not less than 48 h and examined for changes in homogeneity and color [19, 29].

Viscosity measurements and rheological behavior

The viscosity of the optimized nanoemulsion was determined using Brookfield Cup and Bob Viscometer at 25 °C using small sample adapter and spindle no. 63 at 150 rpm [30].

Degree of transparency (% transmittance)

Transparency of nanoemulsion was evaluated by diluting at $100\times$ and $250\times$ with purified water and analyzing the percent transmittance at 638.2 nm with purified water as blank [19].

Incorporation of nanoemulsion in gel system

LGE and GOR containing nanoemulsion were o/w type of emulsion; therefore, aqueous gelling agents were screened. Gelling agents such as Pemulen TR-1 NF, Carbopol 974P NF, and Ultrez 10 NF were selected for preparation of nanoemulgel. Nanoemulsion was loaded in 0.5%, 0.75%, and 1% wt concentration of these gelling agents. Based on viscosity, texture, and appearance, 0.75% wt Ultrez-10 NF was selected in formulation of nanoemulgel. To prepare NE loaded gel, weighed amount of Ultrez 10 NF was hydrated for 2 h in purified water (in half quantity of the aqueous phase of nanoemulsion) by stirring it on magnetic stirrer. LGE and GOR were added to oil mix, followed by addition of S-mix and remaining aqueous phase. Furthermore, nanoemulsion was then gradually added to the gel with gentle mixing to avoid excessive air entrapment. Finally, triethanolamine (TEA) was used as a pH-adjusting agent to adjust the pH in the range of 5–6 in order to achieve maximum viscosity and form a homogenous, clear gel [31].

Evaluation and characterization of nanoemulsion loaded gel

pH determination

Topical gel must be safe and non-irritating to avoid allergic reactions. Since, pH of the formulation plays a significant role leading to allergic reactions. Hence, pH measurement of nanoemulgels is essential. Nanoemulgel pH was measured by dispersing 5 g of gel in 50 ml of purified water (10% w/w dispersion) at 25 °C using a digital pH meter calibrated at pH 4.2, 7.0, and 9.4 buffers prior to use (Labman Instruments) [32].

Spreadability

One gram of optimized nanoemulgel was sandwiched between two glass slides (i.e., ground slide and upper slide affixed with a hook). Two hundred grams of weight was kept for 5 min on the top to remove excess air and ensure uniform film of the nanoemulgel. A weighed quantity (30 g) was kept on a pan (38 g) that was attached to the pulley. The required time (in seconds) by the glass to slip off from the nanoemulgel in the direction of certain load was recorded. The spreadability of the nanoemulgel is inversely proportional to the time required

for complete separation of glass slides [33, 34]. Spreading was calculated using the mathematical formula.

$$S = m * l/s$$

where S is the spreadability, m is the weight placed in the pan (40 g), l is the length of glass slides (10 cm), and t is the time required in seconds.

Active phytoconstituents determination

Ginger oleoresin consists of 6-gingerol (6-GIN) and lipid guggul extract consists of E-guggulsterone (E-GGS) and Z-guggulsterone (Z-GGS) as active phytoconstituents. The concentration of GOR and LGE in NE was determined by using RP-HPLC. One gram of NE was diluted with 10 ml methanol. After appropriate dilutions with mobile phase (ACN:methanol:water—70:10:20) and the concentration of 6-gingerol (GOR), E- and Z-guggulsterones (LGE) were determined using RP-HPLC [35].

In vitro diffusion study

The in vitro diffusion of optimized gel batch was determined using Franz diffusion cell on nylon membrane of 0.45 μm. The membrane was pre-soaked in the release media and flanked by receptor and donor compartment. The receptor compartment was filled with phosphate buffer pH 7.4:ethanol $(1{:}1) + 3\%$ w/w Tween 80 (release media) in isothermal condition (37 °C $\pm$ 2 °C) and stirred magnetically at 100 rpm. The aliquots were withdrawn at predetermined time intervals and quantified by the developed RP-HPLC method. The samples were replenished with fresh media after removing the aliquots. Percent cumulative release was calculated and plotted against time [36].

Ex vivo diffusion study

The ex vivo diffusion of with optimized gel batch was performed using Franz diffusion cell on porcine ear skin. No animals were harmed during procurement of the porcine ear skin as it was collected from a government-approved abattoir. After sacrificing the animal, the membrane was pre-soaked in the release media and flanked by receptor and donor compartment. The receptor compartment was filled with release media in isothermal condition (37 °C $\pm$ 2 °C) and stirred magnetically at 100 rpm. The aliquots were removed at predetermined time intervals and quantified by the developed RP-HPLC method. The samples were replenished with fresh media after removing the aliquots. Percent cumulative release was calculated and plotted against time. The permeation profile was constructed by calculating the quantity of active phytoconstituents permeated per square centimeter of skin (mcg/

cm^2) versus time (h). The steady state flux (Jss, mcg/cm²h) was calculated from the slope of the linear portion of the plot using linear regression analysis [36–38].

Release kinetics model

Based on the in vitro and ex vivo diffusion studies, various mathematical models were applied to determine the release kinetics of the active compounds from the optimized formulation. The release data was fitted into various equation for zero-order release, first-order release, Higuchi release, and Korsmeyer-Peppas release [37].

Differential scanning colorimetry

The change in physical properties and temperature of the optimized nanoemulsion was determined using DSC method. The sample was heated in the range of 30–500 °C in an aluminum pan that was sealed with perforated lids.

Hen's Egg Test-Chorioallantonic Membrane (HET-CAM) study

HET-CAM is a rapid and sensitive procedure to predict skin irritancy by evaluation of the changes in the CAM of the fertilized eggs. CAM comprises of complete laminate vascular system with arteries, veins, and capillaries that are sensitive to harmful and corrosive substances with an inflammatory process. As per the ICCVAM-recommended test method protocol, the irritation potential of LGE+GOR formulations was evaluated by the HET-CAM assay [39]. Fertile White Leghorn chicken eggs weighing 50 to 60 g were obtained from Central Poultry Development Organization, Mumbai. Nine-day-old, fertilized eggs which were incubated in an automatic rotating machine at 37.5 ± 0.5 °C and 62.5 ± 7.5% RH were utilized for the experimentation. The experimentation method was validated using 0.1 N NaOH (negative control), 0.9% NaCl (positive control), and 0.75% w/w Ultrez-10 NF (gelling agent). The skin irritant property of LGE+GOR NEG was compared to LGE, GOR, LGE+GOR mixture, LGE+GOR NE, and a commercial product (1.16% w/w diclofenac emulgel). The irritating impact was observed visually for 5 min after 0.3 ml of test solutions was applied to the CAM. The irritation score (IS) was determined using the following equation after recording the length of time and extent of injuries following the addition of each sample:

$$IS = \frac{(301 - tH) * 5}{300} + \frac{(301 - tL) * 7}{300} + \frac{(301 - tC) * 9}{300}$$

where tH, tL, and tC are time (in seconds) required for the occurrence of haemolysis, lysis, and coagulation, respectively. Depending on the IS values, formulations were classified as mentioned below non-irritating (IS < 0.9), mildly irritating

$(1.0 \leq IS \leq 4.9)$, moderately irritating $(5.0 \leq IS \leq 8.9)$, or severely irritating $(9.0 \leq IS \leq 21.0)$. The experimentation was performed in triplicate [40, 41].

Cytotoxicity study on RAW 264.7 cells

The in vitro cytotoxicity study was determined by performing MTT assay in RAW 264.7 cell lines. Cells at a density of 2×10^4 were seeded into 96-well microtiter plates (Sigma, Germany) in complete RPMI medium (200 µl per well) and incubated at 37 °C under an atmosphere of 5% CO_2 overnight. Cells were treated with the test compounds (GOR, LGE, and LGE+GOR (1:1)) and diclofenac at 0.5 µg/ml, 1 µg/ml, 2 µg/ml, 10 µg/ml, 20 µg/ml, and 40 µg/ml for 72 h. This was followed by addition of 0.5 mg/ml MTT solution in each well and incubated for 3 h at 37 °C. Later, MTT solution was replaced with 100 µl of dimethyl sulfoxide (DMSO) (MilliporeSigma) for solubilizing the purple formazan crystals. The absorbance was recorded using an ELISA microplate reader (BioTek Synergy H1 Multimode Reader, USA) at λ max = 570 nm and 630 nm [33, 42].

LPS-mediated anti-inflammatory study on RAW 264.7 cells

The RAW cells were seeded at 5×10^5 in a 6-well plate with a volume of 2 ml complete RPMI 1640 medium; furthermore, it was incubated at 37 °C under an atmosphere of 5% CO_2. Cells were then incubated with LPS (1 µg/ml) for 3 h and treated with the test compounds (5% GOR, 5% LGE, 50 µg/ml extract, 5 µg/ml diclofenac, and 2.5% each of GOR and LGE) followed by incubation for 72 h at 37 °C under an atmosphere of 5% CO_2. The cells were harvested in polystyrene tubes and centrifuged at 300 g × g at 25 °C. Cell pellets obtained by centrifugation were washed with PBS after decanting the supernatant. Cells fixation was performed by adding 1 ml of cold 70% ethanol and incubated for 30 min at − 20 °C freezer. This was followed by centrifugation and washing with PBS. Ten microliters of antibodies was added and incubated for 30 min at room temperature in dark condition. Five hundred microliters

Table 1 List of selected Oil-mix based on miscibility

Selected oil-mix	Composition	Ratio
O-1	CO:FO:OA:C-200 P	0.5:0.5:1:1
O-2	CO:FO:OA:C-MCM	0.5:0.5:1:1
O-3	CO:FO:EO:C-200 P	0.5:0.5:1:1
O-4	CO:FO:EO:C-MCM	0.5:0.5:1:1

Table 2 List of selected S-mix based on of miscibility

Selected S-mix	Composition	Ratio
S-1	T-80:K-ELP:TP	1:1:1
S-1A	T-80:K-ELP:TP	0.5:0.5:1
S-2	T-80:K-ELP:PEG-400	1:1:1
S-2A	T-80:K-ELP:PEG-400	0.5:0.5:1
S-3	T-80:K-ELP:PG	1:1:1
S-3A	T-80:K-ELP:PG	0.5:0.5:1

of D-PBS was mixed thoroughly and analyzed by a flow cytometer (FACS-BD Cell quest pro software) [43, 44].

Stability study

Stress studies were performed by subjecting the optimized formulation at numerous temperature conditions. Formulation was packed in sealed glass containers and stored in different temperature zones at 4 ± 3 °C, 25 ± 2 °C/$60 \pm 5\%$ RH, and 40 ± 2 °C/$75 \pm 5\%$ RH for 3 months. At the end of each month, the samples were aliquot for evaluation of any physical change (such as clarity, phase separation, precipitation, and color change), active phytoconstituents concentration, gelling capacity, and pH [45, 46].

In vivo animal study

Complete freund's adjuvant induced arthritic model

The study was carried out in the Department of Pharmacology after the approval of the protocol by the Institutional Animal Ethics Committee (IAEC) (Approval Number — CPCSEA/IAEC/P-4/2020). Male Wistar rats of 180–200 g were procured from National Institute of Biosciences, Pune. Before the commencement of study, animals were acclimatized in laboratory for 2 weeks. Animals were fed with commercial pelleted diet and water ad libitum throughout the experimentation. Complete Freund's adjuvant (CFA) model was opted for studying the efficacy of formulated gel against anti-inflammatory condition [19].

Skin irritation study

Skin irritation was performed by applying LGE+GOR NEG on Wistar rats and evaluated by skin irritation. The dorsal surface of the rats was shaved without damaging the skin surface, 4 h before the application of the respective formulation. The rats were divided into groups each containing six rats: Group1 — positive control; animals were treated as healthy controls; Group 2 — animals were treated with 0.8% v/v aqueous solution of formalin; Group 3 — 1.16% w/w diclofenac emulgel; animals were treated with a commercial product; Group 4 — placebo NEG; animals were treated with placebo nanoemulgel; and Group 5 — LGE+GOR NEG; animals were treated with nanoemulgel containing active phytoconstituents. After application of respective formulation, they were inspected at 24, 48, and 72 h for dermal reactions such as edema or erythema. The mean scores for recorded on the basis of severity caused by application of this formulation: 0—no erythema/edema, 1—slight erythema/edema, 2—moderate erythema/edema, and 3—severe erythema/edema.

Paw edema measurement

The paw edema was measured using digital Vernier caliper on days 0, 7, 14, 21, and 28. Paw edema changes were determined by measuring the difference in paw (in mm) between the initial day and the predetermined days (0, 7th, 14th, 21st, and 28th day).

X-ray analysis

Animals were euthanized on the 28th day and the left hind paws were cut and stored in neutral buffer containing 10% formalin solution. Later, the severity joint and bone deformation were analyzed.

Histopathological analysis

After euthanizing animals, left hind paw was stored in neutral buffer with 10% formalin solution. Joint tissue sections were sliced into 5-μm segments and placed on a glass slide followed
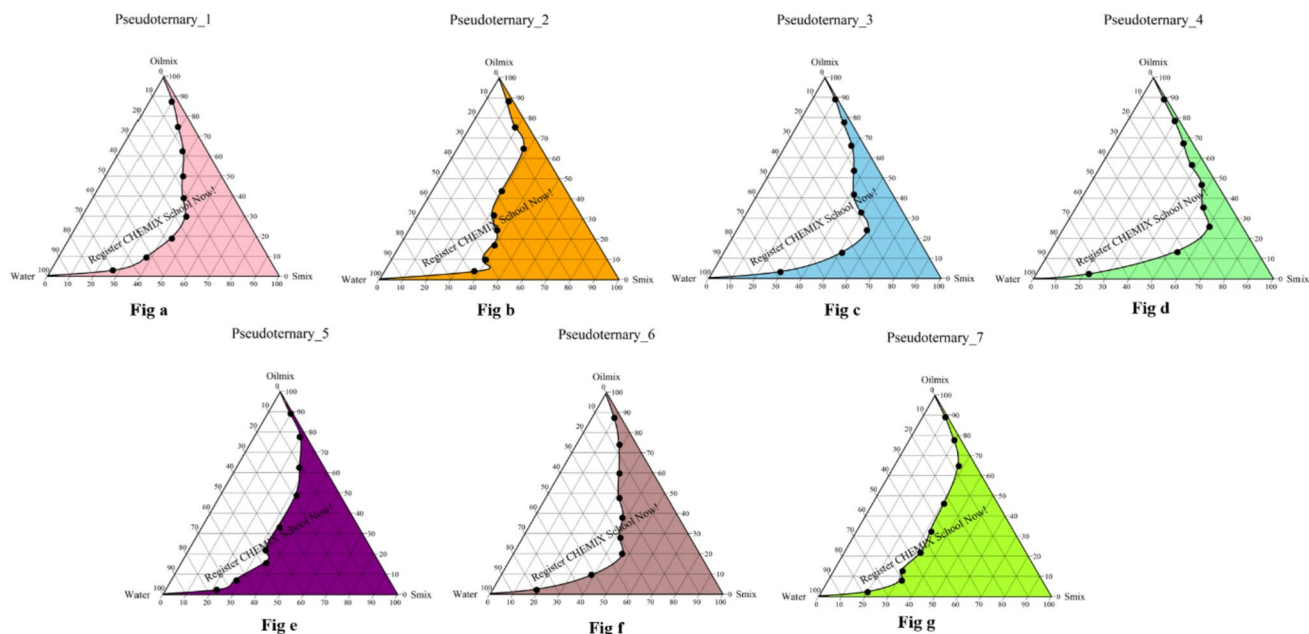
Table 3 List of selected Oil-mix and S-mix combinations for pseudo-ternary phase diagrams

Ternary No.	Oil-mix	S-mix
1	O-1:CO:FO:OA:C-200 P (0.5:0.5:1:1)	S-2A:T-80:K-ELP:PEG-400 (0.5:0.5:1)
2	O-2:CO:FO:OA:C-MCM (0.5:0.5:1:1)	S-3A:T-80:K-ELP:PG (0.5:0.5:1)
3	O-3:CO:FO:EO:C-200 P (0.5:0.5:1:1)	S-2A:T-80:K-ELP:P-400 (0.5:0.5:1)
4	O-4:CO:FO:EO:C-MCM (0.5:0.5:1:1)	S-1A:T-80:K-ELP:TP (0.5:0.5:1)
5	O4:CO:FO:EO:C-MCM (0.5:0.5:1:1)	S-2A:T-80:K-ELP:PEG-400 (0.5:0.5:1)
6	O-1:CO:FO:OA:C-200 P (0.5:0.5:1:1)	S-1B:T-80:K-ELP:TP (1:1:1)
7	O-2:CO:FO:OA:C-MCM (0.5:0.5:1:1)	S-3B:T-80:K-ELP:PG (1:1:1)

Fig. 1 Pseudo-ternary phase diagrams

by staining using hematoxylin and eosin (H&E) sections. Furthermore, the sections were analyzed for cell infiltration, cartilage damage, and bone erosion.

Plasma and synovium IL-6, IL-10, and TNF-α measurements

Blood serum and synovial fluid were collected after the last administration of formulation. Cytokine levels of TNF-α, IL-6, and IL-10 were determined using ELIZA kit [47, 48].

Statistical analysis

One-way analysis of variance (ANOVA) was applied to determine the statistical difference. Cell cytotoxicity was analyzed using Student's t-test with a 95% confidence interval. For all statistical analyses, GraphPad Prism version 7.0 (GraphPad Software, San Diego, CA, USA) was used.

Results and discussion

Selection of oils, surfactants, and co-surfactants

Miscibility studies were carried out to select the most suitable oil phase and aqueous phase. The miscibility of ginger oil and lipid guggul extract was determined my mixing with various oils. Castor oil and fenugreek oil were selected as the functional excipients. The results of the miscibility studies suggest that 4% wt active phytoconstituents mixture (1:1) was completely miscible in all the individual as well as oil mixture. The combination of oil mentioned in Table 1 had the highest emulsification ability. The ratio of castor oil and fenugreek oil to other oils was kept 0.5:0.5:1:1 as increasing its concentration led to instability and turbidity in the system. Similarly, the following ratios of surfactant and co-surfactant, mentioned in Table 2, were used for the development of nanoemulsion.

Table 4 Trail batches containing 2% w/w active phytoconstituents mixture (1:1)

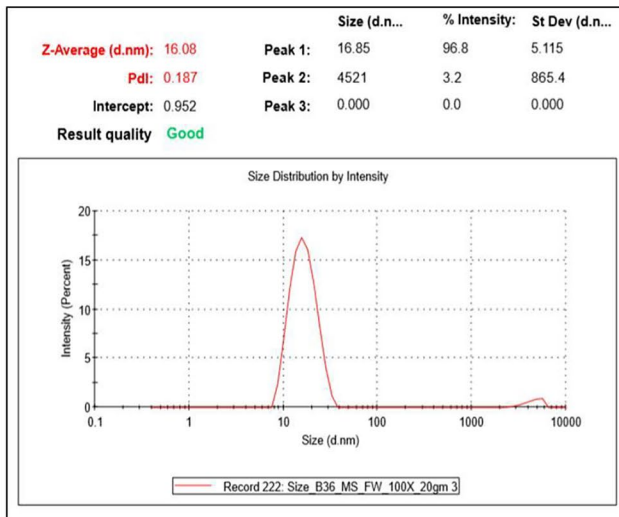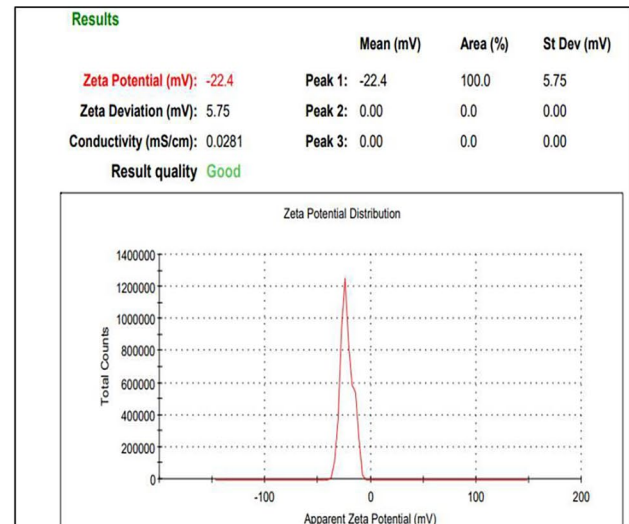| Batch No.	Oil (%)		Surfactant (%)		Millipore water (%)	Observation
1	O-2	10	S-5A	40	48	Clear
2	O-3	10	S-4A	45	43	Clear
3	O-4	10	S-1A	50	38	Clear
4	O-4	10	S-4A	40	48	Clear
5	O-1	5	S-1B	45	48	Clear
6	O-2	10	S-5B	40	48	Clear

Fig. 2 Particle size analysis and zeta potential graph of optimized batch

Formulation and development

Formulation of nanoemulsion was carried out using pseudo-ternary phase diagrams. Construction of the pseudo-ternary diagram is important for determining the concentration of each component to form a stable NE system. Pseudo-ternary diagrams were constructed from the selected Oil-mix and S-mix (mentioned in Table 3) to identify the o/w nanoemulsion region. The pseudo-ternary diagrams with various weight ratios of S-mix (0.5:0.5:1 and 1:1:1) were constructed, while keeping the Oil-mix ratios constant as shown in Fig. 1. Pseudo-ternary diagrams indicated low area for nanoemulsion in Oil-mix containing CO, FO, OA, and C-200P compared to nanoemulsion region of Oil-mix containing CO:FO:OA:C-MCM, and CO:FO:EO:C-MCM. The S-mix contained surfactants in different ratios (0.5:0.5:1 and 1:1:1); however, the phase diagrams did not show any significant difference in the nanoemulsion region. The nanoemulsion batches were

formulated depending on the nanoemulsion region from the phase diagrams. Based on the pseudo-ternary, different batches of nanoemulsion were developed and depending on the observation 6 batches were selected for further characterization and development. Trial batches of nanoemulsion containing 2% w/w are illustrated in Table 4.

Droplet size, polydispersity index, and zeta potential

The mean globule size of all the nanoemulsion was found to be between 18.03 ± 2.55 and 72.56 ± 54.56 nm and PDI was below 0.4 (shown in Fig. 2). For topical drug delivery, the ideal mean globule size is less than 200 nm, with a PDI less than 1.0. The smaller the mean globule size, the larger the surface area which is suitable for rapid pore transport. Zeta potential is an indication of surface charges which contributes in providing stability of the formulation. All the nanoemulsion prepared had a negative zeta potential in the range of -8 to -23 mV indicating their ability to avoid

Table 5 Characterization of nanoemulsion batches

| Batch No.	Zeta size (nm)	PDI	Zeta potential (mV)	% Transmittance		Thermodynamic stability		
				100×	250×	Centrifugation	Heat-cool	Freeze-thaw
1	21.41 ± 0.02	0.269 ± 0.008	-15.1 ± 0.24	98.47	98.47	Passed	Passed	Passed
2	20.67 ± 0.02	0.153 ± 0.010	-12.5 ± 0.48	99.544	99.944	Passed	Passed	Passed
3	25.39 ± 0.04	0.342 ± 0.007	-14.7 ± 0.22	95.177	101.132	Passed	Passed	Passed
4	22.73 ± 0.02	0.220 ± 0.060	-18.1 ± 0.11	97.789	101.102	Passed	Passed	Passed
5	23.76 ± 54.5	0.632 ± 0.05	-15 ± 0.21	97.526	100.941	Passed	Passed	Passed
6	16.08 ± 2.55	0.187 ± 0.06	-22.4 ± 0.31	96.51	99.974	Passed	Passed	Passed
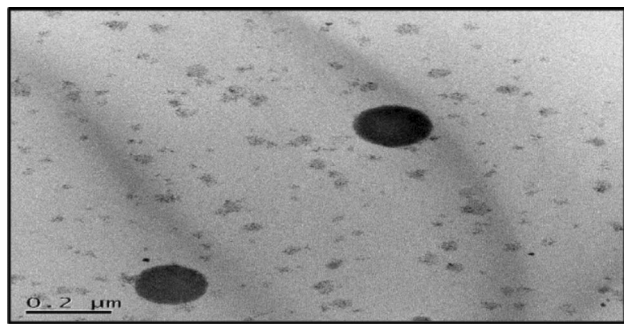
Fig. 3 TEM image of nanoemulsion at 200-nm scale

agglomeration and maintain interfacial boundary of the globules resulting into enhanced stability of nanoemulsion. The results of droplet size, PDI, and ZP are highlighted in Table 5. Also, the TEM image of the developed nanoemulsion is shown in Fig. 3.

Thermodynamic stability and % transmittance

The formulated batches were further investigated for thermodynamic stability by performing centrifugation, heat-cool cycle, and freeze-thaw cycle. The results are shown in Table 5. The batches were found to be thermodynamically stable as they could withstand centrifugation, heat-cool cycle, and freeze-thaw cycle. Percentage transmittance of nanoemulsion was found to be between 95.77 ± 0.05 and $99.54 \pm 0.19\%$ at $100 \times$ dilution and more than 99.49 at $250 \times$ dilution.

Incorporation of nanoemulsion in gel system

Nanoemulsion was further incorporated into various carbopol gel systems such as 0.5%, 0.75%, and 1% wt Carbopol 974P NF, Ultrez-10 NF, and Pemulen TR-1 respectively. Formulation with Carbopol 974P was viscous but

was least clear (turbid) as compared to the other gelling agents. On the other hand, formulation with Pemulen TR-1 had a gritty texture and less viscosity as compared to Ultrez-10 NF. Formulation with Ultrez-10 NF was clear and homogeneous but 0.75% wt Ultrez-10 NF had the optimum viscosity along with clarity and homogeneity; it was selected as the gelling agent.

Determination of pH, viscosity, spreadability, and active content

The mean pH of the active phytoconstituents loaded nanoemulgel was 5–6 (slightly acidic) which indicates compatibility of the gels with the skin surface, i.e., no skin irritation or inflammation is expected with skin. Spreadability measurements were performed based on the slip and drag characteristics of the nanoemulgel, which is an indirect method to determine the gel's uniform spreadability and applicability on the skin. The spreadability of all formulation was between 17 and 26 g cm/s. The viscosity of all the developed batches is highlighted in Table 6. The active phytoconstituents of all the selected nanoemulsion batches were found to be within the range of 90–110%. The active phytoconstituents in batch 6 were found to be 105.28 ± 4.78, 103.50 ± 2.14, and 94.32 ± 3.14 of 6-gingerol, E-GGS, and Z-GGS respectively.

In vitro diffusion study

In vitro diffusion study of batch 6 loaded gel was performed in release media using Franz diffusion cell using nylon membrane (0.45 μm). At 24th h (Fig. 4a), around $99.72 \pm 3.47\%$, $57.98 \pm 2.11\%$, and $86.42 \pm 5.13\%$ of 6-GIN, E-GGS, and Z-GGS respectively were released from the gel matrix. However, in the case of nanoemulsion, the release was faster, and at 8th h, around 80% of the actives were released. Therefore, it can be stated that incorporation of nanoemulsion in gel matrix ensures controlled drug delivery.

Table 6 Characterization of nanoemulgel

Batch No.	pH ($n = 3$)	Spreadability (g cm/s)	Viscosity (cps)	% Actives content in nanoemulgel		
				6-Gingerol	E-GGS	Z-GGS
1	5.46 ± 0.02	18.7 ± 1.32	32.86 ± 0.41	107.27 ± 2.47	90.69 ± 3.68	98.06 ± 1.17
2	5.20 ± 0.03	19.87 ± 1.07	35.8 ± 1.46	97.64 ± 1.25	100.99 ± 2.11	107.1 ± 2.74
3	5.42 ± 0.02	21.4 ± 1.54	36.3 ± 0.1	101.72 ± 1.96	92.45 ± 5.48	99.32 ± 3.18
4	5.53 ± 0.05	17.2 ± 0.98	39.7 ± 0.98	108.36 ± 3.98	96.34 ± 3.77	94.67 ± 2.96
5	5.48 ± 0.03	17.63 ± 2.47	35.63 ± 6.82	97.92 ± 2.51	98.74 ± 2.21	104.26 ± 2.65
6	5.34 ± 0.04	22.41 ± 1.71	38.8 ± 3.21	105.28 ± 4.78	103.50 ± 2.16	94.32 ± 3.14
7	5.53 ± 0.01	25.4 ± 1.21	35.63 ± 1.75	98.90 ± 2.27	101.13 ± 1.25	106.49 ± 0.98

In-vitro drug diffusion from nanoemugel

Fig no. a

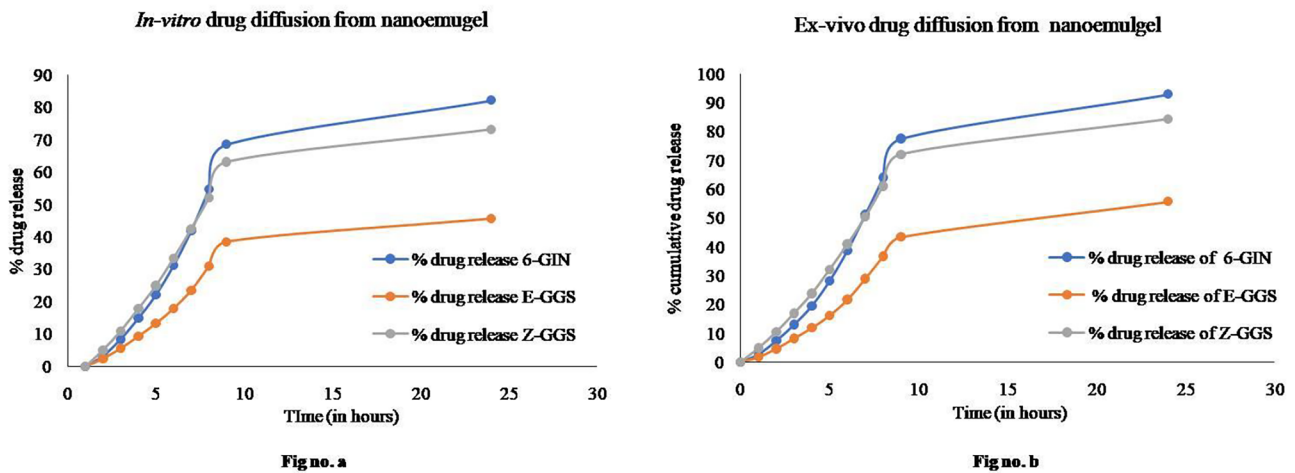**Ex-vivo drug diffusion from nanoemulgel**

Fig no. b

Fig. 4 **a** In vitro release and **b** ex vivo release from nanoemulgel

Ex vivo diffusion study

Ex vivo diffusion study of Batch No. 6 loaded gel (1 g) was performed in release media using Franz diffusion cell using porcine ear skin as membrane. At 24th h, around $92.8 \pm 3.21\%$, $55.61 \pm 0.91\%$, and $84.2 \pm 4.22\%$ of 6-GIN, E-GGS, and Z-GGS respectively were released from the gel matrix. In ex vivo study, diffusion of active phytoconstituents was found to be less as compared to in vitro diffusion which can be attributed to presence of fatty layer in porcine ear. The graphical representation of ex vivo diffusion study is shown in Fig. 4b. The permeation coefficient of 6-GIN, E-GGS, and Z-GGS was found to be 0.233 cm^2/h, 0.135 cm^2/h, and 0.201 cm^2/h respectively.

Release kinetics model

Release kinetics and permeation mechanism from the optimized GOR+LGE NE loaded gel were analyzed using kinetic models such as zero order, first order, Higuchi model, and Korsmeyer-Peppas. In the case of in vitro diffusion, overall curve fitting showed Korsmeyer-Peppas with R^2 of 0.8790 for GOR (6-GIN) and 0.9669 and 0.9868 for LGE

(E-GGS and Z-GGS) respectively. Based on the R^2 value, the types of release kinetic are identified. In the case of ex vivo diffusion, overall curve fitting showed Korsmeyer-Peppas with R^2 of 0.8743 for GOR (6-GIN) and 0.9582 and 0.9855 for LGE (E-GGS and Z-GGS) respectively. Table 7 represents the regression coefficient for in vitro and ex vivo diffusion. It was observed that the GOR has Korsmeyer-Peppas type of release kinetics, whereas LGE showed zero-order release. These results suggest that the active phytoconstituents demonstrated controlled release.

Differential scanning colorimetry

DSC thermogram of gingerol, lipid guggul extract, and mixture of gingerol and lipid guggul extract is shown in Fig. 5a–c. As per the DSC thermograms, GOR and LGE show exothermic peaks at 383.0 °C and 392.5 °C respectively. Figure 5c shows endothermic peaks at 389.7 °C and 400.3 °C which corresponds to peaks of GOR and LGE respectively. Figure 5f indicates the DSC overlay which does not show the presence of endothermic peak of both actives and was identical to the thermogram of placebo

Table 7 Release kinetics for optimized nanoemulgel in in vitro and ex vivo diffusion study

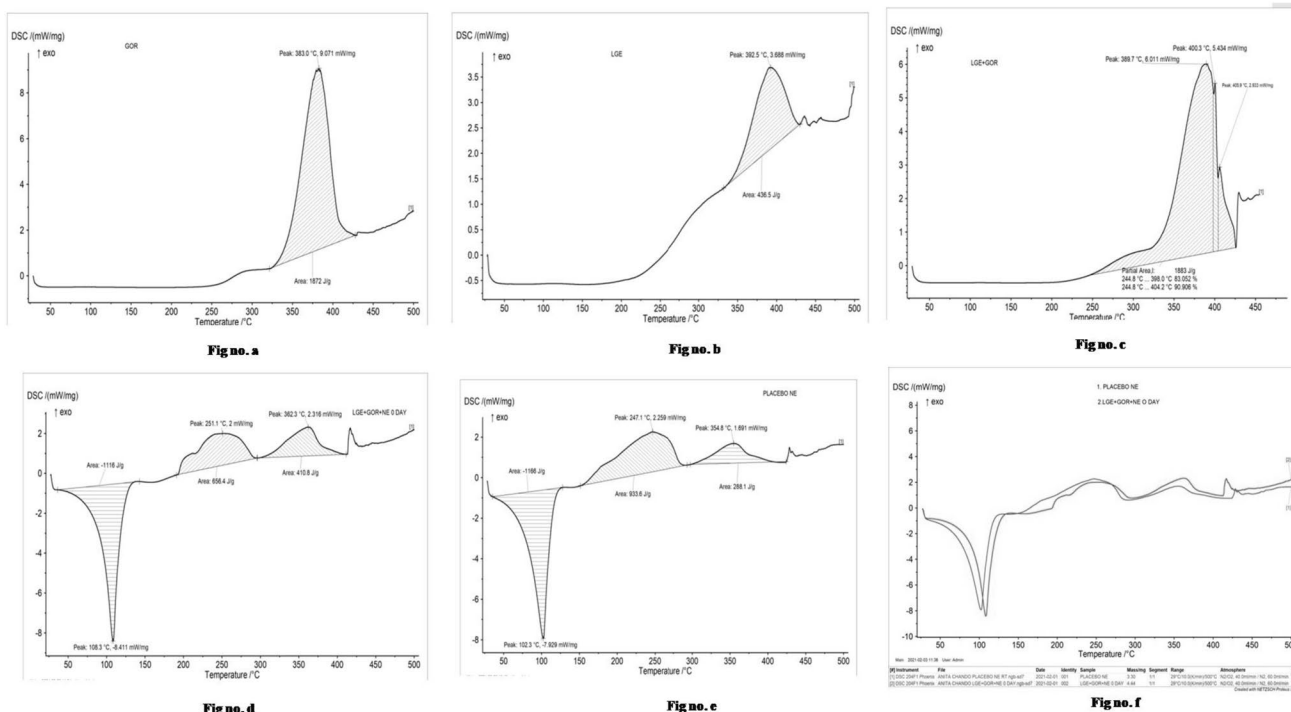|		6-GIN (R^2)	E-GGS (R^2)	Z-GGS (R^2)
In vitro diffusion	Zero order	0.7813	0.9669	0.9868
	First order	0.831	0.8104	0.7656
	Higuchi	0.8605	0.8064	0.8491
	Korsmeyer-Peppas	0.879	0.9692	0.9032
Ex vivo diffusion	Zero order	0.7745	0.9582	0.9855
	First order	0.831	0.8136	0.7665
	Higuchi	0.8512	0.789	0.8455
	Korsmeyer-Peppas	0.8743	0.9883	0.9083

Fig. 5 DSC images. **a** Gingerol. **b** Lipid guggul extract. **c** Mixture of gingerol and lipid guggul extract. **d** Placebo. **e** Actives loaded NGE. **f** Overlay of placebo and actives loaded NGE

nanoemulsion. Therefore, it can be concluded that the actives were completely encapsulated in the lipidic phase.

Hen's Egg Test-Chorioallantonic Membrane (HET-CAM) study

As mentioned in Table 8 and shown in Fig. 6, the nanoemulgel was found to be non-irritating and non-sensitizing in nature as compared to pure actives conventional gel and marketed formulation (diclofenac emulgel) which has slight irritation potential. This suggests that encapsulation of these actives in nanocarriers such as nanomemulsion could be an effective way to reduce skin irritation possessed by pure extracts.

Stability study

The final formulation was charged for stability for 3 months and then evaluated with respect to physical appearance, pH, globule size, zeta potential and actives content. The results mentioned in Table 9 indicates that the formulation is stable. Also, the variations in evaluated parameters indicated the results were not statistically significant ($p > 0.05$).

Cytotoxicity study on RAW 264.7 cells

Figure 7 shows % cell viability of 25% GOR, LGE, LGE+GOR, and diclofenac on RAW 264.7 cells. The

Table 8 Comparative evaluation of various formulation w.r.t level of skin irritation

| Compounds	IS score (mean ± SD)	Irritation level
Negative control (0.9% NaCl)	0.00	No irritation
Positive control (0.1 N NaOH)	11.996 ± 0.001	Severe irritation
Vehicle (olive oil)	0.00	No irritation
0.75% Carbopol Ultrez 10 NF	0.00	No irritation
1% LGE solution	2.144 ± 0.1456	Slight irritation
1% GOR solution	6.51 ± 0.0467	Moderate irritation
1%LGE+1% GOR solution	7.088 ± 0.116	Moderate irritation
Placebo NEG	0.00	No irritation
1% LGE+1% GOR NEG	0.00	No irritation
1.16% w/w diclofenac sodium emulgel	3.118 ± 0.0486	Slight irritation
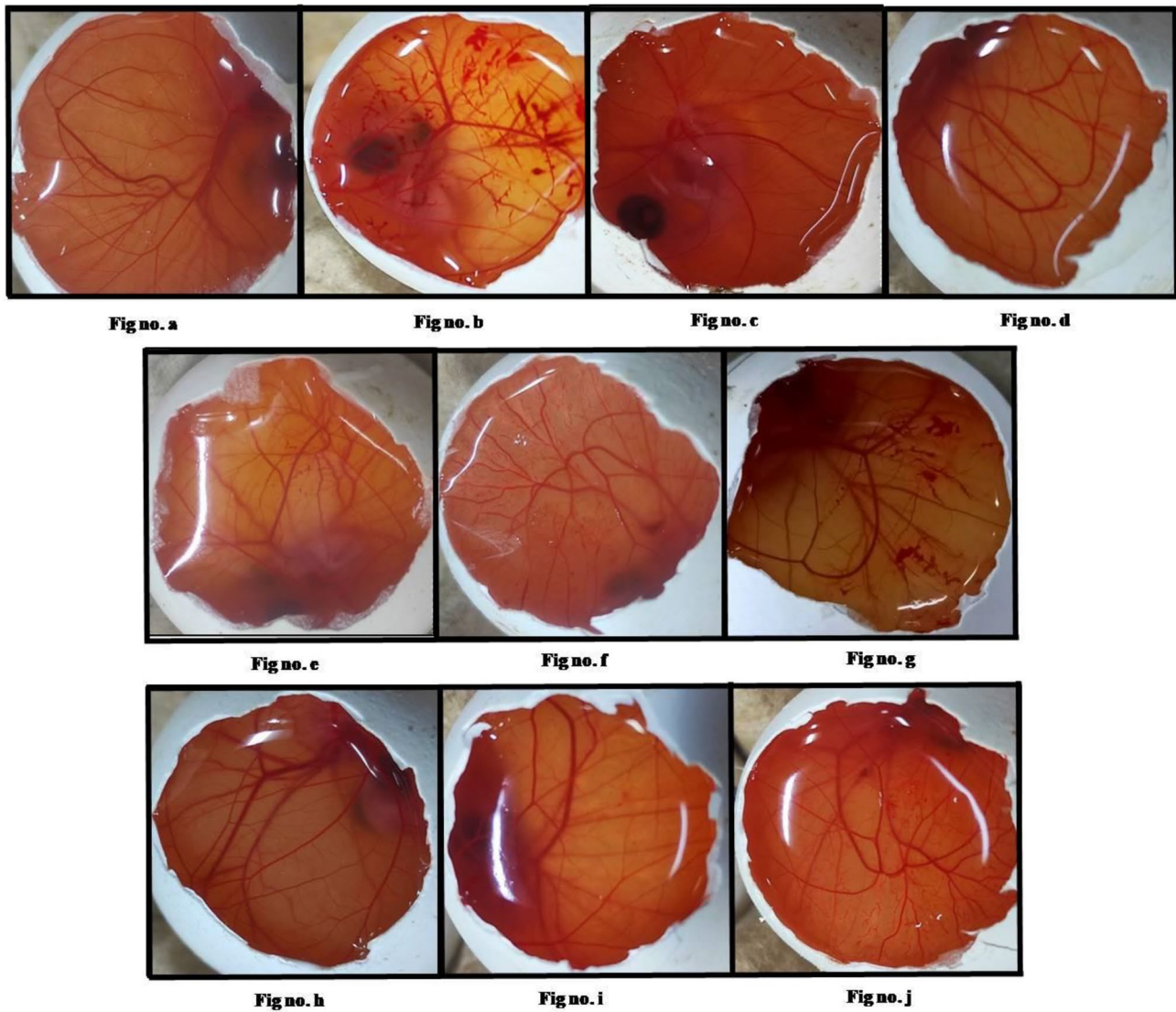
Fig. 6 HET CAM images. **a** Negative control (0.9% NaCl). **b** Positive control (0.1 N NaOH). **c** Vehicle (olive oil). **d** 0.75% Carbopol Ultrez 10 NF. **e** 1% LGE solution. **f** 1% GOR solution. **g** 1%LGE+1% GOR solution. **h** Placebo NEG. **i** 1% LGE+1% GOR NEG. **j** Diclofenac sodium emulgel

Table 9 Three months stability study data

Sr. No.	Parameter		Day 0	After 3 months		
				At 4 °C	At ambient temperature	At 45 °C
1	Physical appearance		Yellow and clear	Yellow and clear	Yellow and clear	Yellow and clear
2	pH		5.34 ± 0.02	5.34 ± 0.01	5.32 ± 0.03	5.36 ± 0.02
3	Globule size		18.03 ± 2.55	18.98 ± 3.49	18.20 ± 2.43	19.12 ± 2.87
4	Zeta potential		-22.4 ± 5.75	-20.2 ± 4.62	-21.60 ± 2.87	-18.2 ± 7.86
5	% of active phytocompounds	6-GIN	105.28	104.12	105.12	103.21
		E-GGS	103.5	102.87	103.37	102.36
		Z-GGS	99.32	99.06	99.08	98.36
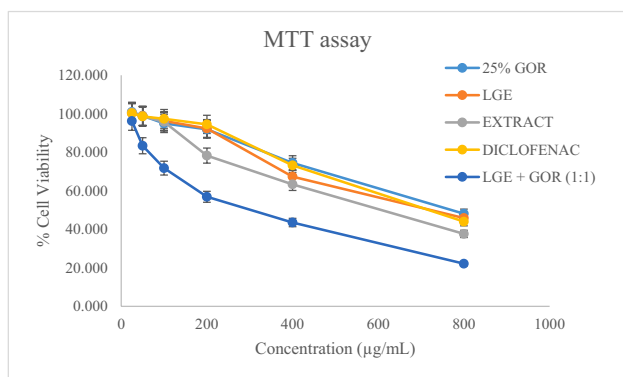
Fig. 7 MTT assay of 25% GOR, LGE, extract, diclofenac, and LGE+GOR (1:1)

results of MTT assay suggest that the IC50 values of 25% GOR, LGE, LGE+GOR, and diclofenac on RAW 264.7 cells were 39.06 ± 0.34, $36.1 \pm 0.55\%$, 19.74 ± 0.13, and 36.73 µg/ml respectively.

LPS-mediated anti-inflammatory study on RAW 264.7 cells

LPS-mediated anti-inflammatory studies were performed on RAW 264.7 cells to determine the levels of the cytokines IL-6, IL-10, and TNF-α. Figure 8 depicts % of cells stimulated with LPS expressing the cytokines IL-6, IL-10, and TNF-α after treating with various test compounds. LPS-induced cells treated with either GOR or LGE did not show improvement in the expression of cytokine level. It is evident

from the graph that treatment with GOR and LGE expressed cytokines similar to diclofenac. Also, the cells treated with GOR-LGE NEG showed significant decrease in the levels of the anti-inflammatory cytokines IL-6 and TNF-α and increase in the pro-inflammatory cytokine IL-10. Therefore, it can be stated that the combination of LGE and GOR incorporated into nanoemulsion can be used for the treatment in reducing the anti-inflammatory activity.

Complete Freund's adjuvant induced arthritis model

On day 0, 0.1 ml of CFA was injected into the left hind paw's sub-plantar region to cause RA in Wistar rats. The ankle width measurements were conducted prior and after 24 h of induction. Paw edema and body weight were monitored on a weekly basis, i.e., on days 1, 7, 14, 21, and 28 day of the induction. Blood withdrawal was done on day 28 for TNF-α, IL-6, and IL-10 estimation in rat blood plasma. Paw was separated from the animal for X-ray and histopathological analyses after sacrificing them.

Skin irritation studies

The topical application should be free from skin irritation and sensitivity reactions. In this, it was observed that LGE and GOR loaded nanoemulgel did not show any severe skin irritation. Symptoms such as edema and erythema during 72 h of observation as compared to diclofenac emulgel showed slight irritation of skin. Therefore, it was concluded that the optimized nanoemulgel is non-irritating, non-sensitizing, and safe for topical use.

Fig. 8 Cytokine expression of IL-6, IL-10, and TNF-α in LPS-induced cells

Fig. 9 Paw edema measurement of CFA-induced rats treated with diclofenac emulgel, placebo NEG, and LGE+GOR NEG. Note: A statistically significant difference in the paw edema in rats treated with LGE+GOR NEG nanoemulgel; $p < 0.05$. *$p < 0.05$ represents a significant difference when compared with negative control. #$p < 0.05$ represents significant difference when compared with placebo group
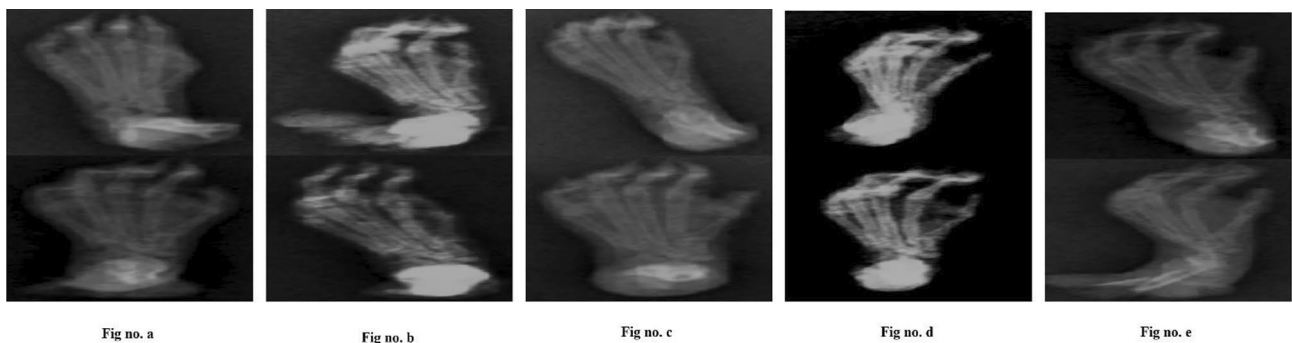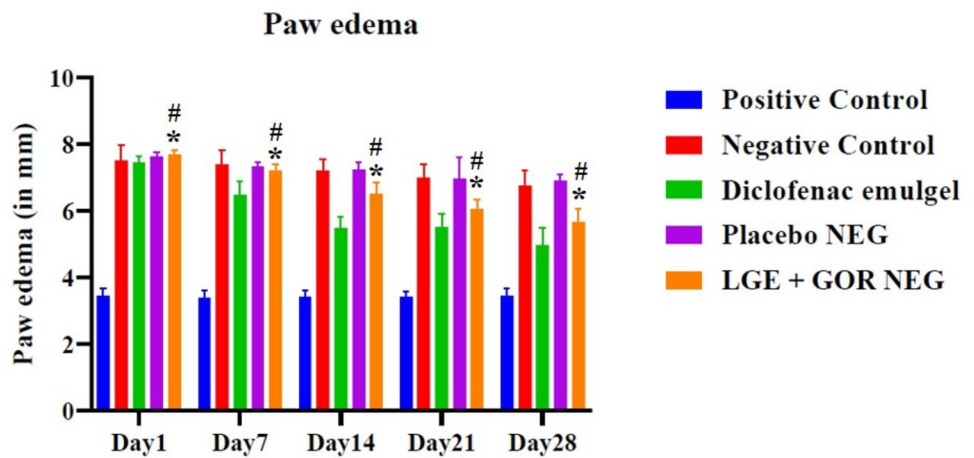

Fig. 10 X-ray of left hind paw of CFA induced rats. **a** Positive control. **b** Negative control. **c** Diclofenac nanoemugel. **d** Placebo NEG. **e** LGE+GOR NEG

Paw edema measurement

The measurement of the paw edema was done using a digital vernier caliper. Paw edema measured on days 1, 7, 14, 21, and 28 (shown in Fig. 9) indicated that LGE+LGE NEG and diclofenac sodium emulgel showed significant reduction in the edema on the 28th day after the treatment as compared to the negative control and placebo groups.

X-ray analysis

Radiographic examination of the paw from the positive control group (shown in Fig. 10) showed the normal joint without distension and normal joint space radio density. Animals from the negative control and placebo nanoemulgel groups showed arthritic changes such as increase joint radio density and narrowing in joint space were observed. However, the
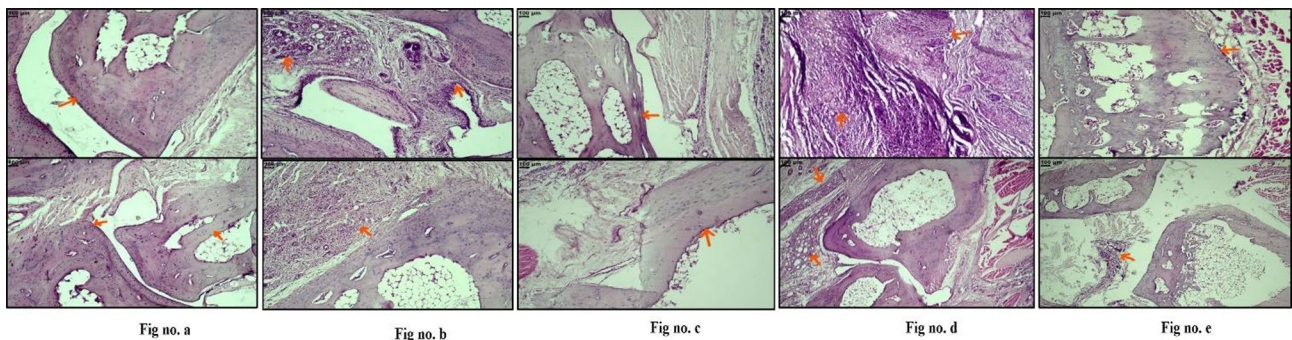
Fig. 11 Histopathological evaluation of left hind paw of CFA induced rats. **a** Positive control. **b** Negative control. **c** Diclofenac nanoemugel. **d** Placebo NEG. **e** LGE+GOR
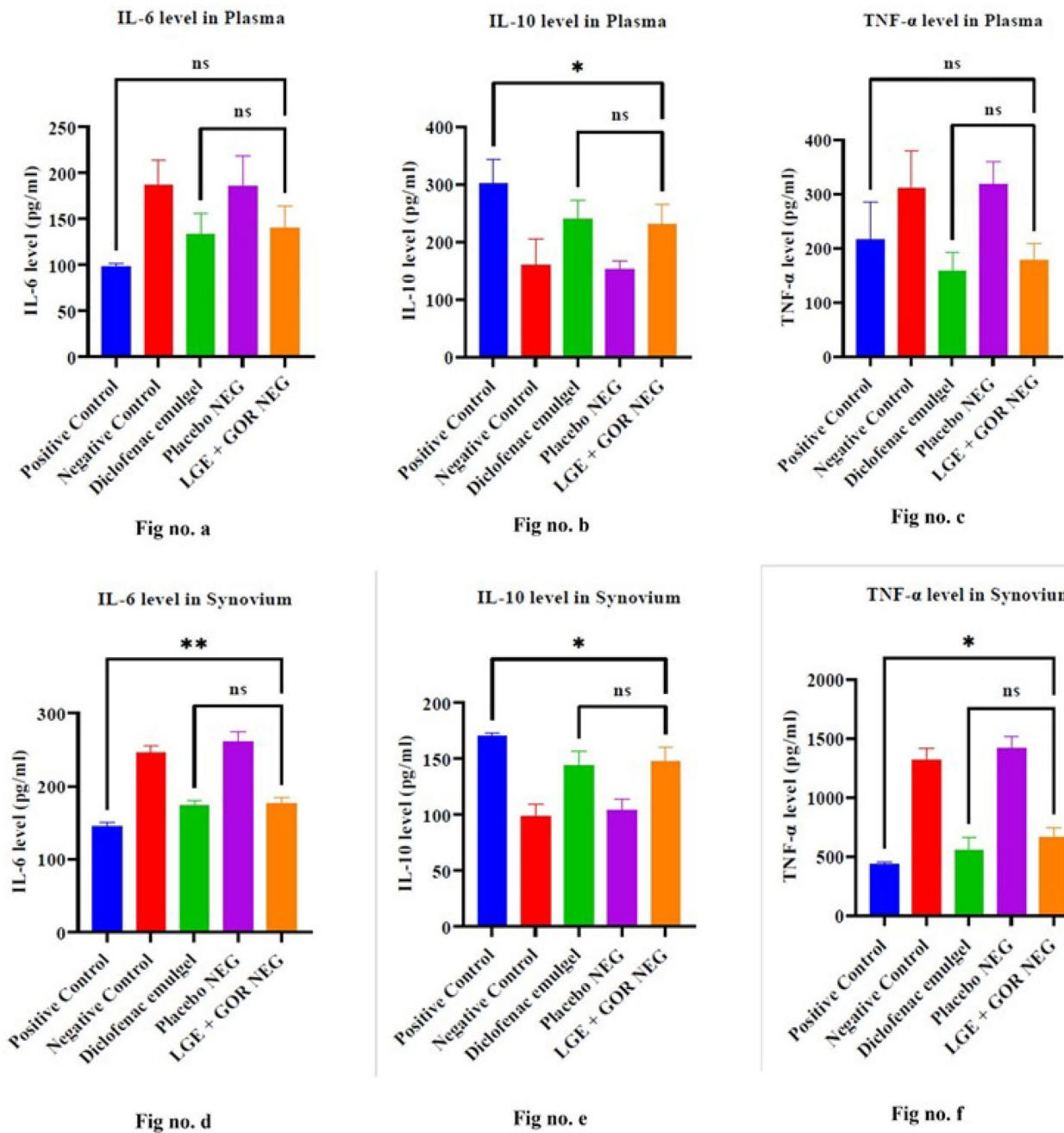
Fig. 12 Cytokine levels in plasma and synovium of CFA-induced rats observed after 28 days of treatment. **a** IL-6 in plasma. **b** IL-10 in plasma. **c** TNF-α in plasma. **d** IL-6 in synovium, **e** IL-10 in syn-ovium. **f** TNF-α in plasma. Note: ns, non significant ($p > 0.05$). *Significant ($p \leq 0.05$), **very significant ($p \leq 0.01$)

severity and intensity were reduced in the LGE+GOR NEG group and diclofenac Na emulgel group. The joint space and radio density were comparable between the diclofenac emulgel group and LGE+GOR NEG group suggestive of good anti-inflammatory and anti-arthritic properties.

Histopathology study

In Fig. 11, microscopic examination of paw showed normal bone tissue in the positive control group of animals. Animals from negative control and placebo nanoemulgel showed

inflammatory changes such as infiltration of inflammatory cells and minimal erosion in bone when compared with the control group. However, animals from the diclofenac Na emulgel and LGE+GOR nanoemulgel groups showed decreased in the severity of inflammatory cells. Based on histopathology findings, it can be concluded animal treated with diclofenac Na emulgel and LGE+GOR nanoemulgel showed decrease in the severity and incidence of these changes indicating of anti-arthritic effects.

Estimation of IL-6, TNF-α, and IL-10 in blood plasma and synovium

IL-6 and TNF-α are anti-inflammatory cytokines prominently present during the progression of RA. It was observed that LGE+GOR NEG and diclofenac sodium emulgel reduced the IL-6 and TNF-α levels more than the positive and placebo NEG in plasma and synovium. Similar results were observed with the anti-inflammatory cytokine IL-10. The graphical representation of the data is shown in Fig. 12. Therefore, LGE+GOR NEG can be used as an effective alternative for management of pain and inflammation associated with rheumatoid arthritis.

Conclusion

In conclusion, the present work was focused to develop GOR and LGE nanoemulgel for the treatment for rheumatoid arthritis. In vitro studies suggested that active phytoconstituents loaded nanoemulgel exhibited a slow and prolonged release of the both actives. Based on HET-CAM, it can be stated that the formed nanoemulgel had no skin irritation ability as compared to diclofenac emulgel which showed slight irritation in both studies. Therefore, nanoemulsion can be an efficient technique in encapsulating the actives with irritating potential. During the preclinical studies, it was observed that active phytoconstituents loaded nanoemulgel had better efficacy in terms ofreduction of inflammation of the paw edema which was supported by histopathological and X-ray analyses. IL-6 and TNF-α levels in plasma were found to reduce and the levels of IL-10 in actives loaded nanoemulgel and diclofenac emulgel. Therefore, ginger oleoresin and lipid guggul extract-based nanoemulgel can be potential candidates for further studies as a new efficient treatment in patients with rheumatoid arthritis.

Declarations

References

1. Guo Q, Wang Y, Xu D, Nossent J, Pavlos NJ, Xu J. Rheumatoid arthritis: pathological mechanisms and modern pharmacologic therapies. Bone Res. 2018;6:15.

2. Kemble S, Croft AP. Critical Role of Synovial Tissue-Resident Macrophage and Fibroblast Subsets in the Persistence of Joint Inflammation. Front Immunol. 2021;12:715894.

3. Anita C, Munira M, Mural Q, Shaily L. Topical nanocarriers for management of Rheumatoid Arthritis: A review. Biomed Pharmacother. 2021;141:111880.

4. Almoallim H, Al Saleh J, Badsha H, Ahmed HM, Habjoka S, Menassa JA, et al. A Review of the Prevalence and Unmet Needs in the Management of Rheumatoid Arthritis in Africa and the Middle East. Rheumatol Ther. 2021;8:1–16.

5. Nilsson J, Andersson M, Hafström I, Svensson B, Forslind K, Ajeganova S, et al. Influence of Age and Sex on Disease Course and Treatment in Rheumatoid Arthritis. OARRR. 2021;13:123–38.

6. Saxena A, Raychaudhuri SK, Raychaudhuri SP. Rheumatoid Arthritis: Disease Pathophysiology. Inflammation, Advancing Age and Nutrition: Research and Clinical Interventions. 2013;215–29.

7. Shehu S, Kurya AU, Aliyu U, Sharma DC. Role of inflammatory cytokines in the pathogenesis of rheumatoid arthritis and novel therapeutic targets. Asian J Immunol. 2020;4(2).

8. Deane KD, Holers VM. Rheumatoid Arthritis Pathogenesis, Prediction, and Prevention: An Emerging Paradigm Shift. Arthritis Rheumatol. 2021;73:181–93.

9. Gómez-Bañuelos E, Mukherjee A, Darrah E, Andrade F. Rheumatoid Arthritis-Associated Mechanisms of Porphyromonas gingivalis and Aggregatibacter actinomycetemcomitans. JCM. 2019;8:1309.

10. Köhler G, Kaudewitz L. Current therapeutic options in the treatment of rheumatoid arthritis. JCM. 2019;8(7):938.

11. Lindler BN, Long KE, Taylor NA, Lei W. Use of Herbal Medications for Treatment of Osteoarthritis and Rheumatoid Arthritis. Medicines. 2020;7:67.

12. Ballester P, Cerdá B, Arcusa R, Marhuenda J, Yamedjeu K, Zafrilla P. Effect of Ginger on Inflammatory Diseases. Molecules. 2022;27:7223.

13. Jayanudin, Fahrurrozi M, Wirawan SK, Rochmadi. Preparation of Chitosan Microcapsules Containing Red Ginger Oleoresin Using Emulsion Crosslinking Method. J App Biomater Function Mater. 2019;17:228080001880991.

14. Bhardwaj M, Alia A. Commiphora wightii (Arn.) Bhandari. Review of Its Botany, Medicinal Uses, Pharmacological

Activities and Phytochemistry. J Drug Delivery Ther. 2019;9:613–21.

15. Bhat MH, Fayaz M, Kumar A, Jain AK. Chemistry and Pharmacology of Guggulsterone: An Active Principle of Guggul Plant. In: Ozturk M, Hakeem KR, editors. Plant and Human Health, (Volume 3, p. 301–19). Cham: Springer International Publishing; 2019. https://doi.org/10.1007/978-3-030-04408-4_14. Cited 7 Apr 2023.

16. Arianto A, Cindy C. Preparation and Evaluation of Sunflower Oil Nanoemulsion As a Sunscreen. Open Access Maced J Med Sci. 2019;7:3757–61.

17. Bashir M, Ahmad J, Asif M, Khan S-U-D, Irfan M, Y Ibrahim A, et al. Nanoemulgel, an Innovative Carrier for Diflunisal Topical Delivery with Profound Anti-Inflammatory Effect: in vitro and in vivo Evaluation. IJN. 2021;16:1457–72.

18. Basudkar V, Gharat SA, Momin MM, Shringarpure M. A Review of Anti-Aging Nanoformulations: Recent Developments in Excipients for Nanocosmeceuticals and Regulatory Guidelines. Crit Rev Ther Drug Carrier Syst. 2022;39:45–97.

19. Gokhale JP, Mahajan HS, Surana SJ. Quercetin loaded nanoemulsion-based gel for rheumatoid arthritis: In vivo and in vitro studies. Biomed Pharmacother. 2019;112:108622.

20. Sharma B, Iqbal B, Kumar S, Ali J, Baboota S. Resveratrol-loaded nanoemulsion gel system to ameliorate UV-induced oxidative skin damage: from in vitro to in vivo investigation of antioxidant activity enhancement. Arch Dermatol Res. 2019;311:773–93.

21. Sindhu G, Shyni GL, Pushpan CK, Nambisan B, Helen A. Evaluation of anti-arthritic potential of Trigonella foenum graecum L. (Fenugreek) mucilage against rheumatoid arthritis. Prostaglandins Other Lipid Mediat. 2018;138:48–53.

22. Ladani M. Brief review on analgesic and anti-inflammatory properties of Moringa oleifera, Senna auriculata & other useful medicinal plants to inhibit release of immune mediators. Int J Herbal Med. 2022;10(3):33–8.

23. Kheawfu K, Pikulkaew S, Rades T, Müllertz A, Okonogi S. Development and characterization of clove oil nanoemulsions and self-microemulsifying drug delivery systems. J Drug Deliv Sci Technol 2018;46:330–8.

24. Sharma P, Tailang M. Design, optimization, and evaluation of hydrogel of primaquine loaded nanoemulsion for malaria therapy. Futur J Pharm Sci. 2020;6:26.

25. Arora R, Aggarwal G, Harikumar SL, Kaur K. Nanoemulsion Based Hydrogel for Enhanced Transdermal Delivery of Ketoprofen. Adv Pharm. 2014;2014:1–12.

26. Mohammed NK, Muhialdin BJ, Meor Hussin AS. Characterization of nanoemulsion of Nigella sativa oil and its application in ice cream. Food Sci Nutr. 2020;8:2608–18.

27. Pathan I, Mangle M, Bairagi S. Design and Characterization of Nanoemulsion for Transdermal Delivery of Meloxicam. Anal Chem Lett 2016;6:286–95.

28. Sharma N, Kaur G, Khatkar SK. Optimization of emulsification conditions for designing ultrasound assisted curcumin loaded nanoemulsion: Characterization, antioxidant assay and release kinetics. LWT. 2021;141:110962.

29. Donthi MR, Saha RN, Singhvi G, Dubey SK. Dasatinib-Loaded Topical Nano-Emulgel for Rheumatoid Arthritis: Formulation Design and Optimization by QbD, In Vitro, Ex Vivo, and In Vivo Evaluation. Pharmaceutics. 2023;15:736.

30. Pereira Oliveira CN, Nani Leite M, de Paula NA, Araújo Martins Y, Figueiredo SA, Cipriani Frade MA, et al. Nanoemulsions Based on Sunflower and Rosehip Oils: The Impact of Natural and Synthetic Stabilizers on Skin Penetration and an Ex Vivo Wound Healing Model. Pharmaceutics. 2023;15:999.

31. Lala RR, Awari NG. Nanoemulsion-based gel formulations of COX-2 inhibitors for enhanced efficacy in inflammatory conditions. Appl Nanosci. 2014;4:143–51.

32. Gostyńska A, Czerniel J, Kuźmińska J, Brzozowski J, Majchrzak-Celińska A, Krajka-Kuźniak V, et al. Honokiol-Loaded Nanoemulsion for Glioblastoma Treatment: Statistical Optimization, Physicochemical Characterization, and an In Vitro Toxicity Assay. Pharmaceutics. 2023;15:448.

33. Gharat S, Basudkar V, Momin M, Prabhu A. Mucoadhesive Oro-Gel–Containing Chitosan Lipidic Nanoparticles for the Management of Oral Squamous Cell Carcinoma. J Pharm Innov. https://doi.org/10.1007/s12247-023-09724-7. Cited 7 Apr 2023.

34. Mutimer MN, Riffkin C, Hill JA, Glickman ME, Cyr GN. Modem Ointment Base Technology II.:Comparative Evaluation of Bases. J Am Pharm Assoc (Scientific ed). 1956;45:212–8.

35. Latif MS, Nawaz A, Asmari M, Uddin J, Ullah H, Ahmad S. Formulation Development and In Vitro/In Vivo Characterization of Methotrexate-Loaded Nanoemulsion Gel Formulations for Enhanced Topical Delivery. Gels. 2022;9:3.

36. Algahtani MS, Ahmad MZ, Ahmad J. Nanoemulgel for Improved Topical Delivery of Retinyl Palmitate: Formulation Design and Stability Evaluation. Nanomaterials. 2020;10:848.

37. Morsy, Abdel-Latif, Nair, Venugopala, Ahmed, Elsewedy, et al. Preparation and Evaluation of Atorvastatin-Loaded Nanoemulgel on Wound-Healing Efficacy. Pharmaceutics. 2019;11:609.

38. Nagaraja S, Basavarajappa GM, Attimarad M, Pund S. Topical Nanoemulgel for the Treatment of Skin Cancer: Proof-of-Technology. Pharmaceutics. 2021;13:902.

39. Interagency Coordinating Committee on the Validation of Alternative Methods (ICCVAM). Recommended Test Method Protocol: Hen ' s Egg Test – Chorioallantoic Membrane (HET-CAM) Test Method. ICCVAM Test Method Evaluation Report. 2010;13:B30–8.

40. Alvarez-Rivera F, Fernández-Villanueva D, Concheiro A, Alvarez-Lorenzo C. α-Lipoic Acid in Soluplus ® Polymeric Nanomicelles for Ocular Treatment of Diabetes-Associated Corneal Diseases. J Pharm Sci. 2016;105:2855–63.

41. Anantaworasakul P, Chaiyana W, Michniak-Kohn BB, Rungseevijitprapa W, Ampasavate C. Enhanced Transdermal Delivery of Concentrated Capsaicin from Chili Extract-Loaded Lipid Nanoparticles with Reduced Skin Irritation. Pharmaceutics. 2020;12:463.

42. Suresh P, Salem-Bekhit MM, Veedu HP, Alshehri S, Nair SC, Bukhari SI, et al. Development of a Novel Methotrexate-Loaded Nanoemulsion for Rheumatoid Arthritis Treatment with Site-Specific Targeting Subcutaneous Delivery. Nanomaterials. 2022;12:1299.

43. Qiu J-G, Mei X-L, Chen Z-S, Shi Z. Cytokine Detection by Flow Cytometry. In: Vancurova I, editor. Cytokine Bioassays (p. 235–42). New York, NY: Springer New York; 2014. Available from: https://doi.org/10.1007/978-1-4939-0928-5_21. Cited 8 Apr 2023.

44. Soni JM, Sardoiwala MN, Choudhury SR, Sharma SS, Karmakar S. Melatonin-loaded chitosan nanoparticles endows nitric oxide synthase 2 mediated anti-inflammatory activity in inflammatory bowel disease model. Mater Sci Eng C. 2021;124:112038.

45. Rehman A, Iqbal M, Khan BA, Khan MK, Huwaimel B, Alshehri S, et al. Fabrication, In Vitro, and In Vivo Assessment of Eucalyptol-Loaded Nanoemulgel as a Novel Paradigm for Wound Healing. Pharmaceutics. 2022;14:1971.

46. Sultan MH, Javed S, Madkhali OA, Alam MI, Almoshari Y, Bakkari MA, et al. Development and Optimization of Methylcellulose-Based Nanoemulgel Loaded with Nigella sativa Oil for Oral Health Management: Quadratic Model Approach. Molecules. 2022;27:1796.

47. Kimmerling KA, Gomoll AH, Farr J, Mowry KC. Amniotic Suspension Allograft Modulates Inflammation in a Rat Pain Model of Osteoarthritis. J Orthop Res. 2020;38:1141–9.

48. Pandey S, Rai N, Mahtab A, Mittal D, Ahmad FJ, Sandal N, et al. Hyaluronate-functionalized hydroxyapatite nanoparticles laden

with methotrexate and teriflunomide for the treatment of rheumatoid arthritis. Int J Biol Macromol. 2021;171:502–13.